

Structural phase transition in substituted La_2CuO_4 and $\text{Pr}_2\text{CuO}_{4-y}$

MEENA CHAUDHRI, KUNAL B MODI*, K M JADHAV and G K BICHILE

Department of Physics, Dr. B.A.M. University, Aurangabad 431 004, India

*Department of Physics, Saurashtra University, Rajkot 360 005, India

MS received 30 April 1996; revised 23 October 1996

Abstract. The structural phase transition from orthorhombic (T) phase to tetragonal (T') phase in substituted $\text{La}_{2-x}\text{R}_x\text{CuO}_4$ (R = Pr, Nd, Sm, Eu and Gd) and T' to T-phase in $\text{Pr}_{2-x}\text{M}_x\text{CuO}_{4-y}$ (M = Sr, Ca) has been studied by X-ray diffraction technique. The T-phase of La_2CuO_4 is transferred to T' phase abruptly at $x = 0.8, 0.4, 0.4, 0.3$ and 0.4 respectively for substitution of Pr, Nd, Sm, Eu and Gd for La in La_2CuO_4 without evidence of the T* phase. The T' structure of Pr_2CuO_4 ($x = 0.0$) gets transformed to the T* structure at 30% Ca doping ($x = 0.6$) and then to the T structure at 50% Ca doping ($x = 1.0$), while for Sr-content $x = 0.0, 0.4$ and 1.0 it shows T', T* and T structure respectively.

Keywords. Superconductor; phase transition; X-ray diffraction.

PACS Nos 74·00; 61·10; 64·70

1. Introduction

Since the discovery of high T_c superconductivity [1] in the $\text{La}_{2-x}\text{Ba}_x\text{CuO}_4$ system which has a distorted K_2NiF_4 structure (or the so-called T phase), superconductivity has also been found in two other K_2NiF_4 -related structures, T' and T* phases [2, 3]. The T' phase R_2CuO_4 (R = rare earth) is exhibited by most rare earths whereas the cuprate T phase is found only when R = La. One major difference between the T and T' phases (figure 1) is the coordination of copper. Copper in the T phases has a 6-fold coordination with four of the oxygen atoms in the CuO_2 plane, and the remaining two oxygen atoms (called apical oxygen) above and below the Cu atoms. In contrast, copper in the T' phase is in 4-fold coordination (i.e. no apical oxygen). Intermediate between the T and T' phases is the T* phase. The T* phase has one apical oxygen atom associated with the CuO_5 -square pyramids (figure 1).

The superconductors with T* or T structure are *p*-type (i.e. the carriers are holes) whereas the superconductors with the T' structure are *n*-type (i.e. the carriers are electrons). Finally the T* phase, whole unit cell can be viewed as containing half of the unit cell of the *p*-type T phase and half of the unit cell of *n*-type T' phase, appears as an attractive system in which one could expect, depending on the nature of the chemical doping, to achieve either *p* or *n*-type superconductivity.

To our knowledge, there have been very few studies on such type of systems [2–5]. We considered it interesting to investigate the nature of transition from T-phase to

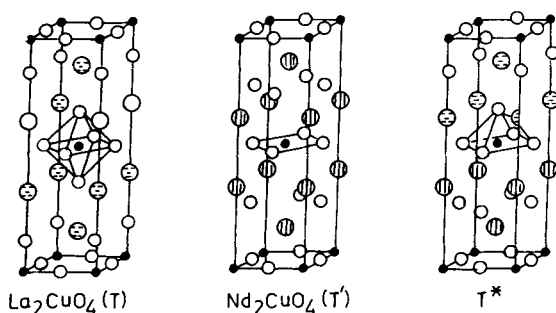


Figure 1. The T-La₂CuO₄, T'-R₂CuO₄ and T*-phases (LaR')CuO₄, (closed circle (●): Cu; open circle (○): oxygen; large circle with hatches (⊕): rare earth ions).

T'-phase by examining their crystal structures. For the present investigations, solid solutions of La_{2-x}R_xCuO₄ (R = Pr, Nd, Sm, Eu and Gd) are prepared.

In view of the appearance of the three possible structural phases T, T' and T* in the divalent substituted 2-1-4 type systems, we have initiated a study on the structural behaviour of pure and Sr and Ca doped Pr_{2-x}M_xCuO_{4-y} system with different concentration (x).

2. Experimental details

All the samples were prepared using standard ceramic method [6]. The samples were characterized by X-ray diffraction using CuK α radiations at room temperature within the 2 θ range of 20° to 50°. The observed X-ray peaks were indexed and analyzed using REFEDT least squares programme, to obtain the values of lattice parameters.

The parent compounds La₂CuO₄, Nd₂CuO₄, Sm₂CuO₄, Pr₂CuO₄, Eu₂CuO₄ and Gd₂CuO₄ and a series of compounds La_{2-x}R_xCuO₄ (R = Pr, Nd, Sm, Eu and Gd) were prepared under identical conditions using the stoichiometric quantities of fine powders of La₂O₃, Pr₆O₁₁, Nd₂O₃, Sm₂O₃, Eu₂O₃, Gd₂O₃ and CuO (all 99.99% pure, Aldrich make). The accurately weighed powders were thoroughly mixed in an agate mortar and pestle and heated at 900°C for 24 h in platinum crucibles. The reacted product was reground and re-heated at 950°C for 24 h to obtain homogeneous, single phase samples. The black product, thus obtained, was pulverized and cold pressed into pellets of uniform thickness by applying suitable pressure. The pellets were then sintered in air at 1000°C for 24 h. The samples were cooled to room temperature at the rate of 2°C/min, during all the heating stages.

Polycrystalline materials of Pr_{2-x}M_xCuO_{4-y} (M = Sr, Ca) with x = 0.0, 0.2, 0.4, 0.6, 0.8 and 1.0 were synthesized by solid state reaction technique [6]. High purity (99.99% pure, Aldrich) dried powders of Pr₆O₁₁, SrCO₃, CaCO₃ and CuO were thoroughly mixed, pelletized and calcined at 950°C in air for 30 min. This short time firing was repeated at least twice. Finally the pellets were sintered at 1080°C in air for 48 h with one intermediate regrinding. These pellets were cooled at a rate of 2°C/min. during all these heating stages. These well sintered pellets were then annealed in ambient oxygen temperature at the rate of 1°C/min. Repeated grinding and short time firing were essential to get homogeneous, single phase materials.

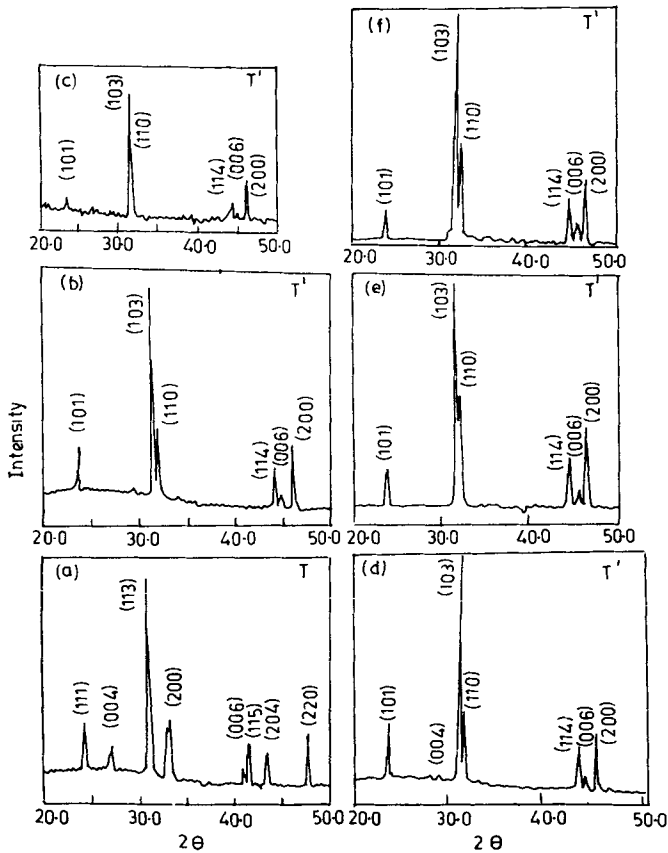


Figure 2. X-ray diffraction patterns of (a) La_2CuO_4 (b) Nd_2CuO_4 (c) Sm_2CuO_4 (d) Pr_2CuO_4 (e) Eu_2CuO_4 and (f) Gd_2CuO_4 systems.

3. Results and discussion

3.1 The $R_2\text{CuO}_4$ compounds ($R = \text{La}, \text{Pr}, \text{Nd}, \text{Sm}, \text{Eu}$ and Gd)

The X-ray diffraction patterns of the parent compounds La_2CuO_4 , Nd_2CuO_4 , Sm_2CuO_4 , Pr_2CuO_4 , Eu_2CuO_4 and Gd_2CuO_4 are shown in figure 2. The absence of extra peaks confirms the phase purity of the samples prepared. The observed X-ray peaks were indexed and values of lattice parameters were calculated using REFEDT least squares programme. The lattice parameters and structure of the above compound are tabulated in table 1. The unit cell parameters agree very well with the reported values [8].

The T' -phase $R_2\text{CuO}_4$ ($R = \text{Pr}, \text{Nd}, \text{Sm}, \text{Eu}$ and Gd) is exhibited by most rare earths were the cuprate T -phase is found only when $R = \text{La}$. The CuO_4 square in the T' -phase is considerably expanded and c axis shrunk, relative to the T -phase structure. This can also be seen from table 1 that there is relative shrunk in c -axis of T' -phase structure with respect to T -phase structure.

Table 1. X-ray data R_2CuO_4 ($R = La, Pr, Nd, Sm, Eu$ and Gd) systems.

System	Lattice parameters		Structure
	$a(\text{\AA})$	$c(\text{\AA})$	
La_2CuO_4	3.797	13.174	T
Pr_2CuO_4	3.969	12.224	T'
Nd_2CuO_4	3.946	12.168	T'
Sm_2CuO_4	3.949	12.061	T'
Eu_2CuO_4	3.924	11.992	T'
Gd_2CuO_4	3.899	11.895	T'

3.2 The $La_{2-x}R_xCuO_4$ ($R = Pr, Nd, Sm, Eu$ and Gd)

Any attempt to induce metallic behaviour in La_2CuO_4 through doping can be achieved only without degrading the critical structural stability. In other words, one cannot reduce the (La–O) bond-length and/or increase the (La–O) bond length upon doping. The substitution of La by any other trivalent rare earths which have smaller ionic radius than La will invariably lead to a reduction in the (R–O) bond-length and thus to an eventual collapse of the T-phase. In pure R_2CuO_4 if R is smaller than La (1.15 Å) then T-phase cannot be stabilized as in the case of other smaller rare earth based 2-1-4 systems with $R = Pr(0.92 \text{ \AA}), Nd(1.08 \text{ \AA}), Sm(1.04 \text{ \AA}), Eu(1.12 \text{ \AA})$ and $Gd(1.02 \text{ \AA})$. Since La_2CuO_4 is already at the critical point of structural instability due to the large tension experienced by the (La–O) bond, one may rotate these bonds by 45° with respect to the (Cu–O) bond to improve the match of (La–O) with (Cu–O) and achieve the atomic arrangement of the T' phase. As a result of this rotation, the (R–O) bond in the T'-phase is under compression in contrast to the T-phase for La_2CuO_4 . Smaller R's are then more favorable for the T'- R_2CuO_4 , consistent with the experimental observations of T'-phase with $R = Pr, Nd, Sm, Eu$ and Gd . For these smaller R's, the oxygen atoms tend to move toward the space between the R-layers due to the stronger attraction associated with R and due to the conservation of charge. Xue *et al* [5] suggested that within the experimental resolution, the (R–O) bond is either under compression and the (Cu–O) bond is either under tension ($R = Nd$ and Pr) or slight compression ($R = Eu$ and Gd) in these compounds.

Thus the substitution of other rare earths smaller than La, for La in La_2CuO_4 system having T-phase structure may lead to T'-phase structure. Thus attempt has been made to gain insight into structural phase transition in T-phase La_2CuO_4 by substituting Pr, Nd, Sm, Eu and Gd for La as a function of concentration (x) in system $La_{2-x}R_xCuO_4$ ($R = Pr, Nd, Sm, Eu$ and Gd).

The X-ray diffraction patterns of $La_{2-x}Pr_xCuO_4$, $La_{2-x}Nd_xCuO_4$, $La_{2-x}Sm_xCuO_4$, $La_{2-x}Eu_xCuO_4$ and $La_{2-x}Gd_xCuO_4$ for different concentration (x) are shown in figures 3 and 4. The values of unit cell parameters, cell volume, c/a ratio and structure obtained from the XRD data for the systems $La_{2-x}Pr_xCuO_4$, $La_{2-x}Nd_xCuO_4$ and $La_{2-x}Sm_xCuO_4$ are presented in table 2 and those for systems $La_{2-x}Eu_xCuO_4$ and $La_{2-x}Gd_xCuO_4$ are tabulated in table 3.

Structural phase transition

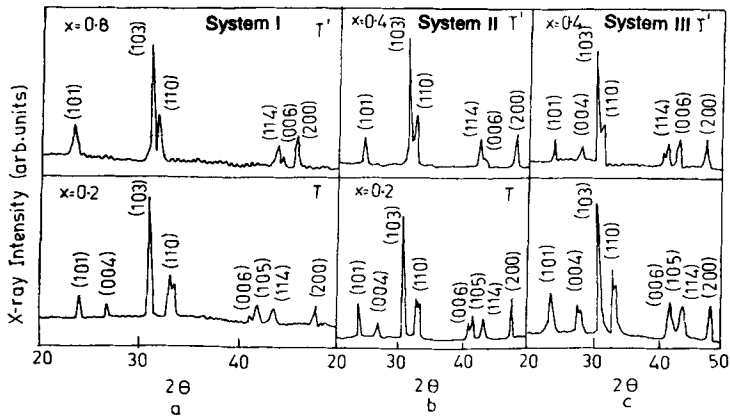


Figure 3. Typical X-ray diffraction patterns of $\text{La}_{2-x}\text{Pr}_x\text{CuO}_4$, $\text{La}_{2-x}\text{Nd}_x\text{CuO}_4$ and $\text{La}_{2-x}\text{Sm}_x\text{CuO}_4$ systems.

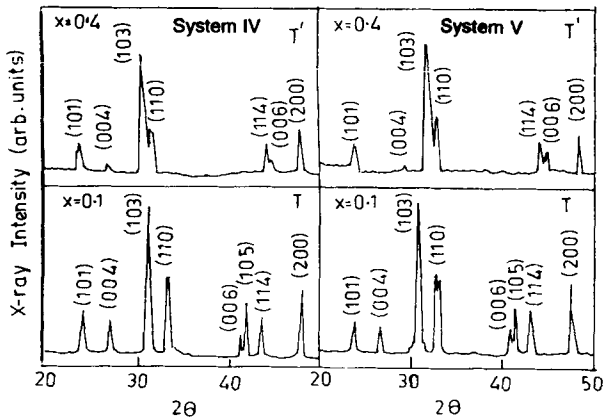


Figure 4. Typical X-ray diffraction patterns of $\text{La}_{2-x}\text{Eu}_x\text{CuO}_4$ and $\text{La}_{2-x}\text{Gd}_x\text{CuO}_4$ systems.

For the system $\text{La}_{2-x}\text{Pr}_x\text{CuO}_4$ the structure remains in the earlier orthorhombic T-phase until $x = 0.6$. For $x > 0.6$, the phase transition from T to T'-phase occurs. For the systems $\text{La}_{2-x}\text{Nd}_x\text{CuO}_4$ and $\text{La}_{2-x}\text{Sm}_x\text{CuO}_4$ the structural phase transition occurs at $x = 0.4$, while for the systems $\text{La}_{2-x}\text{Eu}_x\text{CuO}_4$ and $\text{La}_{2-x}\text{Gd}_x\text{CuO}_4$ at $x = 0.3$ and $x = 0.4$ it shows structural phase transition from orthorhombic T to tetragonal T'-phase.

For all the five systems $\text{La}_{2-x}\text{Pr}_x\text{CuO}_4$, $\text{La}_{2-x}\text{Nd}_x\text{CuO}_4$, $\text{La}_{2-x}\text{Sm}_x\text{CuO}_4$, $\text{La}_{2-x}\text{Eu}_x\text{CuO}_4$ and $\text{La}_{2-x}\text{Gd}_x\text{CuO}_4$ the structural phase transition is accompanied by notable change in cell volume and c/a ratio (tables 2 and 3). This volume change is opposite to the expected view based on the basis of the smaller size of the substituent lanthanide ions; the size effect is apparent only for the values of x larger than the critical values. Since the co-ordination number of both copper and the rare earth ions are lower

Table 2. Lattice parameters, cell volume, c/a ratio and structure of $\text{La}_{2-x}\text{Pr}_x\text{CuO}_4$, $\text{La}_{2-x}\text{Nd}_x\text{CuO}_4$ and $\text{La}_{2-x}\text{Sm}_x\text{CuO}_4$ systems.

Sample x	Lattice parameters		Volume $V(\text{\AA})^3$	c/a	Structure
	$a(\text{\AA}) = b(\text{\AA})$	$c(\text{\AA})$			
$\text{La}_{2-x}\text{Pr}_x\text{CuO}_4$					
0.0	3.797	13.174	189.93	3.469	T
0.2	3.785	13.131	188.32	3.469	T
0.4	3.778	13.137	187.51	3.477	T
0.6	3.735	13.167	183.68	3.525	T
0.8	3.991	12.257	195.23	3.071	T'
1.0	3.969	12.268	193.25	3.090	T'
$\text{La}_{2-x}\text{Nd}_x\text{CuO}_4$					
0.2	3.788	13.162	188.91	3.474	T
0.4	3.998	12.311	196.78	3.079	T'
0.6	3.991	12.332	196.42	3.090	T'
0.8	3.980	12.330	195.31	3.097	T'
1.0	3.976	12.348	195.20	3.105	T'
$\text{La}_{2-x}\text{Sm}_x\text{CuO}_4$					
0.2	3.792	13.119	188.65	3.459	T
0.4	3.983	12.397	196.07	3.112	T'
0.6	3.966	12.336	194.03	3.110	T'
0.8	3.965	12.333	193.89	3.110	T'
1.0	3.961	12.296	192.92	3.104	T'

Table 3. Lattice parameters, cell volume, c/a ratio and structure of $\text{La}_{2-x}\text{Eu}_x\text{CuO}_4$ and $\text{La}_{2-x}\text{Gd}_x\text{CuO}_4$ systems.

Sample x	Lattice parameters		Volume $V(\text{\AA})^3$	c/a	Structure
	$a(\text{\AA}) = b(\text{\AA})$	$c(\text{\AA})$			
$\text{La}_{2-x}\text{Eu}_x\text{CuO}_4$					
0.1	3.801	13.165	190.30	3.463	T
0.2	3.797	13.147	189.55	3.462	T
0.3	3.797	13.113	188.63	3.457	T'
0.4	3.905	12.415	189.32	3.179	T'
0.5	3.895	12.419	188.41	3.188	T'
$\text{La}_{2-x}\text{Gd}_x\text{CuO}_4$					
0.1	3.799	13.174	190.13	3.467	T
0.2	3.799	13.159	189.91	3.464	T
0.3	3.799	13.142	189.68	3.459	T
0.4	3.912	12.183	186.44	3.114	T'
0.5	3.904	12.345	188.15	3.162	T'

in the T' structure than in the T structure, packing would be less efficient in the former, thereby causing increase in cell volume at composition when the structural phase transition occurs.

Structural phase transition

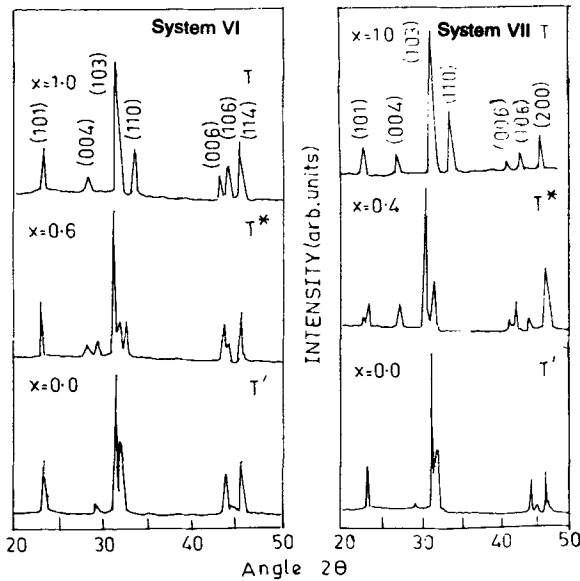


Figure 5. Typical X-ray diffraction patterns of $\text{Pr}_{2-x}\text{Sr}_x\text{CuO}_{4-y}$ and $\text{Pr}_{2-x}\text{Ca}_x\text{CuO}_{4-y}$ systems.

Table 4. Lattice parameters, $c/3a$ ratio and structure of $\text{Pr}_{2-x}\text{Sr}_x\text{CuO}_{4-y}$ and $\text{Pr}_{2-x}\text{Ca}_x\text{CuO}_{4-y}$ systems

Sample	Lattice parameters		$c/3a$	Structure
x	$a(\text{\AA})$	$c(\text{\AA})$		
$\text{Pr}_{2-x}\text{Sr}_x\text{CuO}_{4-y}$				
0.0	3.959	12.224	1.029	T'
0.2	3.956	12.336	1.042	T'
0.4	3.867	12.535	1.080	T*
0.6	3.877	12.506	1.077	T*
0.8	3.866	12.562	1.083	T*
1.0	3.796	12.974	1.139	T
$\text{Pr}_{2-x}\text{Ca}_x\text{CuO}_{4-y}$				
0.0	3.958	12.224	1.029	T'
0.2	3.961	12.227	1.028	T'
0.4	3.969	12.229	1.027	T'
0.6	3.868	12.367	1.065	T*
0.8	3.835	12.217	1.061	T*
1.0	3.752	12.859	1.142	T

Typical XRD patterns of $\text{Pr}_{2-x}\text{Sr}_x\text{CuO}_{4-y}$, with $x = 0.0, 0.4$ and 1.0 are shown in figure 5. The observed X-ray diffraction peaks were modelled by modified Gaussian functions and refined unit cell parameters were calculated using standard least squares programme. The measured values of lattice parameters including the $c/3a$ ratios are listed in table 4. The $c/3a$ ratios were useful to distinguish the three

related T, T' and T* phases [8]. Typical values of $c/3a$ ratio are 1.028, 1.085 and 1.151 for T' (Nd_2CuO_4), [7] T* ($\text{La}_{0.84}\text{Sm}_{0.96}\text{Sr}_{0.2}\text{CuO}_{4-y}$) and T (La_2CuO_4) phases respectively (since La_2CuO_4 forms in an orthorhombically distorted T structure at room temperature, a quasi tetragonal $a(\text{\AA})$ parameter is used to calculate $c/3a$ ratio) [9]. The presence of a structural phase was also confirmed by comparing the observed X-ray patterns with standard patterns reported in the literature [10]. The observed $c/3a$ ratios for $x = 0.0, 0.4$ and 1.0 are consistent with the T', T* and T structures respectively. Also, one can clearly notice these structures from the observed X-ray peaks.

Typical X-ray diffractograms of $\text{Pr}_{2-x}\text{Ca}_x\text{CuO}_{4-y}$ with $x = 0.6$ and 1.0 are shown in figure 5. Table 4 gives the details of the lattice parameters, $c/3a$ ratio and structures. As evident from table 4, the T' structure of Pr_2CuO_4 gets transformed to the T* structure at 30% Ca doping ($x = 0.6$) and then to the T structure at 50% Ca doping ($x = 1.0$).

From table 4 it can be seen that the substitution of Sr for Pr increases the $c(\text{\AA})$ parameters and decreases $a(\text{\AA})$ parameters by 0.75\AA and 0.163\AA . Similarly for Ca substitution also increases the $c(\text{\AA})$ parameters by 0.635\AA and decrease $a(\text{\AA})$ parameters by 0.206\AA for the range studied. Increase in $c(\text{\AA})$ parameters for both Sr and Ca suggest that substituted Sr or Ca for Pr are located along the c -axis.

Thus the X-ray diffraction study on present systems suggest that

- (i) the T-phase La_2CuO_4 is transferred to T'-phase by substitution of La by R (R = rare earth) having smaller ionic radius than La and is accompanied by change in lattice parameters.
- (ii) for the systems $\text{Pr}_{2-x}\text{Sr}_x\text{CuO}_{4-y}$ and $\text{Pr}_{2-x}\text{Ca}_x\text{CuO}_{4-y}$ the divalent (Sr and Ca) substitution for Pr lead to an evolutionary structural phase transformations as $\text{T}' \rightarrow \text{T}^* \rightarrow \text{T}$.

References

- [1] J G Bendnorz and K A Muller, *Z. Phys.* **B64**, 189 (1986)
- [2] Y Tokura, H Takagi and S Uchida, *Nature (London)*, **337**, 345–347 (1989)
- [3] E Takayama Muromachi, Y Matsui, Y Uchida, F Izumi, M Oneda and K Kato, *Jpn. J. Appl. Phys.* **27**, L2283 (1988)
- [4] K K Singh, P Ganguly and C N R Rao, *Mater. Res. Bull.* **17**, 493 (1982)
- [5] Y Y Xue, P H Hor, R L Meng, Y K Tao, Y Y Sun, Z J Hunang, L Gao and C W Chu, *Physica C* **165**, 357 (1990)
- [6] G K Bichile, Smita Deshmukh, D G Kuberkar and R G Kulkarni, *Physica C* **183**, 154 (1991)
- [7] N Nguyen, J Choisnet and B Raveau, *Mater. Res. Bull.* **17**, 567 (1982)
- [8] R Saez Puche, N Norton and W S Glaunsinger, *Mater. Res. Bull.* **17**, 1523 (1982)
- [9] K Takahashi, B Okai, M Kosuga and M Ohta, *Jpn. J. Appl. Phys.* **27**, LI374 (1988)
- [10] H Y Hwang, S W Cheong, A S Cooper, L W Rupp, G H Kwei, Z Tan and B Batlogg, *Physica C* **192**, 362 (1992)